International Journal of Thermophysics, Vol. 20, No. 4, 1999

Contactless Electrical Conductivity Measurement of Electromagnetically Levitated Metallic Melts[1]

T. Richardsen[2] and G. Lohöfer[2, 3]

A facility for noninvasive measurements of the electrical conductivity of liquid metals above and below the melting temperature is presented. It combines the containerless positioning method of electromagnetic levitation with the contactless technique of inductive conductivity measurement. Contrary to the conventional measurement method, the sample is freely suspended within the measuring field and, thus, has no exactly predefined shape. This made a new theoretical basis necessary with implications on the measurement and levitation fields. Furthermore, the problem of the mutual inductive interactions between the levitation and the measuring coils had to be solved.

KEY WORDS: containerless processing; electrical conductivity; electromagnetic levitation; induction; metallic melt; undercooled metallic liquids.

1. INTRODUCTION

The electrical conductivity σ of metallic liquids is of obvious importance to many liquid metal processing operations, because it controls the melt flow under the influence of electromagnetic fields, e.g., during casting processes, or in crystal growth furnaces [1]. Furthermore, via the Wiedemann–Franz law,

$$\frac{\lambda(T)}{\sigma(T)\,T} = L \qquad \text{with} \quad L = 2.45 \times 10^{-8}\ \mathrm{W \cdot \Omega \cdot K^{-2}}$$

a knowledge of the temperature-dependent electrical conductivity $\sigma(T)$ also enables an indirect determination of the temperature dependent thermal

[1] Paper presented at the Fifth International Workshop on Subsecond Thermophysics, June 16–19, 1998, Aix-en-Provence, France.

[2] Institut für Raumsimulation, German Aerospace Center, Linder Höhe, D-51170 Köln, Germany.

[3] To whom correspondence should be addressed.

0195-928X/99/0700-1029$16.00/0

conductivity $\lambda(T)$ of a metallic melt without disturbances by any convective fluid flow in the sample [2].

On the other hand, σ is also a very sensitive indicator for structural changes, like clustering or demixing, etc., within a conducting liquid. And just this fact makes a measurement of σ also in the undercooled melt, i.e., a liquid in the metastable state below its melting temperature, important.

For undercooled metallic melts, where any mechanical contact with the material causes its immediate nucleation, containerless handling methods of the liquid as well as contactless measurement methods are mandatory [3]. Also for liquids above their melting points, especially for high temperatures or reactive materials, only noninvasive techniques can be considered for long-duration measurements. Electromagnetic levitation is an established technique for containerless positioning and heating of metallic melts by means of high-frequency alternating magnetic fields [4, 5]. These levitation fields induce eddy currents in the sample. Their interactions with the original fields produce Lorentz forces, which support the sample against gravity without any mechanical contact.

The noncontact measurement of the electrical conductivity of a liquid or solid material can also be based on electromagnetic induction [6–8]. For this method, the sample is placed in the alternating magnetic field inside of an rf current carrying primary coil of a measuring transformer. The voltage induced in the secondary coil then depends also on the sample conductivity.

We have combined this measurement technique with electromagnetic levitation by placing a pair of measurement coils between the levitation coils. This arrangement causes some problems, however that have to be solved:

- mutual inductive interaction between the levitation and the measurement circuits and
- insufficient knowledge of sample location and sample shape (small asphericities because of magnetic pressure from levitation force field)

In the following we give an overview of our measurement facility and the means by which the different problems are resolved.

2. MEASUREMENT

2.1. Principle

Figure 1 shows the arrangement of our measuring transformer between the levitation coils. When a sample is positioned in the alternating

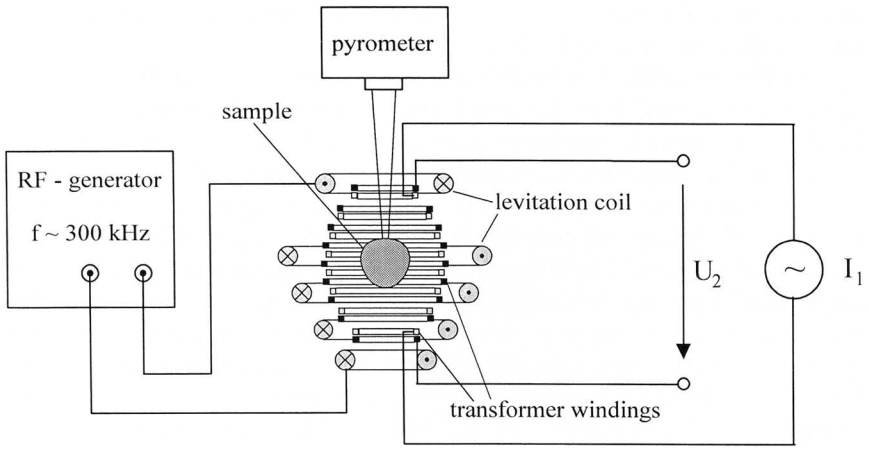

Fig. 1. Schematic diagram of the primary (gray squares) and secondary (black squares) measurement coils integrated within the levitation coil.

magnetic field $B_{\text{coil}} \propto I_1$ generated by the current I_1 in the primary measurement coil, eddy currents are induced in the sample, the strength of which depend on the conductivity σ of the material. These eddy currents generate an additional magnetic rf field $B_{\text{sample}}(\sigma) \propto I_1$. Each of the magnetic fields finally induces a voltage in the secondary measurement coil leading to the total voltage,

$$U_2 = (Z_{\text{coil}} + \Delta Z_{\text{sample}}(\sigma))\, I_1 := Z(\sigma)\, I_1$$

It is evident now that the total impedance $Z(\sigma) = U_2/I_1$, which is the ratio of the two measurable quantities U_2 and I_1, depends on the sample conductivity.

2.2. Procedure

To obtain the conductivity dependent quantity $\Delta Z_{\text{sample}}(\sigma)$, we first measure the voltage U_2 at applied current I_1 without the sample. This yields $Z_{\text{coil}} = U_2/I_1$. Then we repeat this procedure with the sample, which is containerlessly positioned by the levitation field in the center of the measurement transformer, giving $Z(\sigma) = U_2/I_1$. The difference yields

$$\Delta Z_{\text{sample}}(\sigma) = Z(\sigma) - Z_{\text{coil}}$$

The electrical sample conductivity can finally be calculated from the relation between ΔZ_{sample} and σ, which is well known except for calibration constants (see below). In order to determine these calibration constants, we repeat the above mentioned procedure at different current frequencies in the range between 10 kHz and 1 MHz.

During the experiment the alternating current in the primary coil $I_1(t)$, as well as the alternating voltage across the secondary coil $U_2(t)$, is monitored at equal time steps over p periods by a fast data acquisition card. From this set of N data points $\{I_n\}$ and $\{U_n\}$, the complex impedance can be calculated by

$$Z = \frac{\sum_{n=0}^{N} \{U_n[\cos(2\pi p(n/N)) - i\sin(2\pi p(n/N))]\}}{\sum_{n=0}^{N} \{I_n[\cos(2\pi p(n/N)) - i\sin(2\pi p(n/N))]\}}$$

2.3. Evaluation

The measured quantity ΔZ_{sample} depends not only on the electrical conductivity σ but also on the

(a) shape and radius of the sample,

(b) position of the sample within the measurement coils, and

(c) geometry of the measurement coils.

If the measurement coils are designed such that their magnetic fields are nearly homogeneous around the sample, then the dependence of ΔZ_{sample} on the exact sample position disappears and the relation between ΔZ_{sample} and σ simplifies to

$$\Delta Z_{\text{sample}} = ia\omega\mu_0 R_0^3 G(q(\omega, \sigma), \alpha) \tag{1}$$

where μ_0 is the magnetic vacuum permeability (for nonferromagnetic samples), ω is the angular frequency of the fields, and R_0 is the sample radius. Whereas a is a constant which depends on the coil geometry, the function G describes the influence of the sample via the skin depth $\delta(\omega, \sigma)$

$$q(\omega, \sigma) = \frac{R_0}{\delta(\omega, \sigma)}, \qquad \delta(\omega, \sigma) = \sqrt{\frac{2}{\omega\mu_0\sigma}} \tag{2}$$

Weak deviations of the sample from the spherical shape are expressed by the parameter α

$$\alpha = \int_0^{2\pi} \int_0^{\pi} \left(\frac{R(\cos\theta, \varphi) - R_0}{R_0} \right) |Y_1^1(\cos\theta, \varphi)|^2 \sin\theta \, d\theta \, d\varphi$$

which is just the lowest order expansion of the sample surface $R(\cos\theta, \varphi)$ in spherical harmonics. With these quantities the function G is

$$G(q, \alpha) = \frac{1}{3} \frac{j_2((i-1)q)}{j_0((i-1)q)} + \frac{1}{3} \alpha (i-1) q \frac{j_1((i-1)q)}{j_0((i-1)q)} \left(1 + \frac{j_2((i-1)q)}{j_0((i-1)q)} \right) \tag{3}$$

where j_n denotes the nth order spherical Bessel function. For different values of α, Fig. 2 shows the dependence of G on q. For spherical samples ($\alpha = 0$), $G(q, 0)$ has already been derived in Ref. 9.

To get the value of $G(q(\omega, \sigma), \alpha)$ from Eq. (1), we first have to determine the unknown geometry factor a (and possible phase shifts of the data acquisition electronics) by a calibration measurement with a solid spherical sample ($\alpha = 0$) of well-defined conductivity σ and radius R_0. Then ΔZ_{sample}, and thus the value of G, is measured within 0.01 s for about 50 current frequencies between 10 kHz and 1 MHz. Finally, $G(q(\omega, \sigma), \alpha)$, i.e., Eq. (3), as a function of ω is fitted by variation of the unknown parameters σ, R_0, and α at these measurement values, thereby yielding the desired electrical

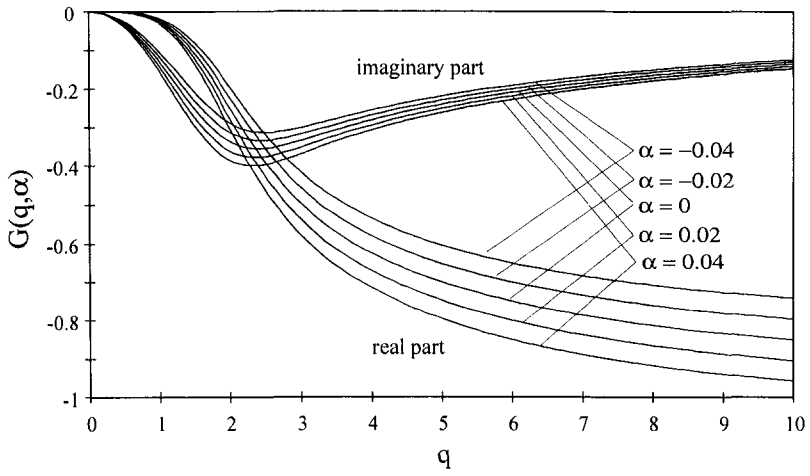

Fig. 2. Graph of the function $G(q, \alpha)$ for different values of the deformation parameter α.

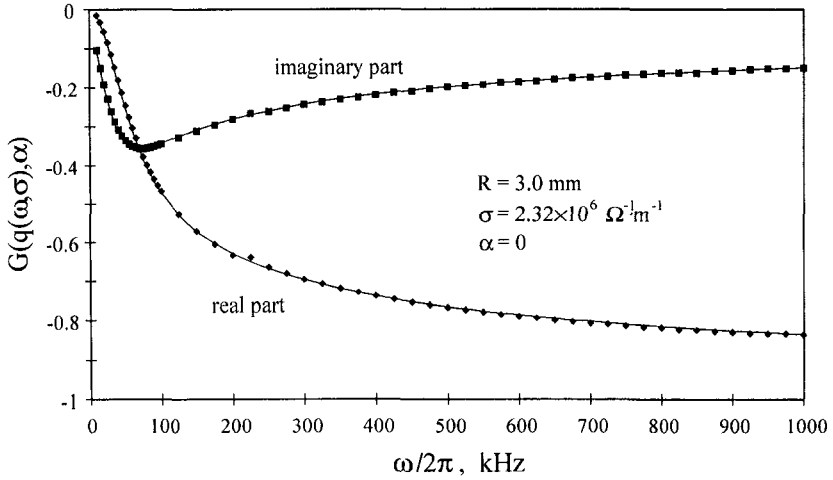

Fig. 3. Data points for a solid, spherical titanium sample at room temperature measured at different frequencies, compared with the theoretical curve.

conductivity σ. A check of this procedure using a solid spherical titanium sample, represented in Fig. 3, shows good agreement between the data points and the fitted theoretical curve.

3. COIL ARRANGEMENT

The relations presented in the preceding section are valid only for

(a) homogeneous measurement fields and

(b) nearly spherical (liquid) samples.

The homogeneity of the measuring field is rendered possible by a special measurement coil geometry, and the nearly spherical shape of the liquid sample by a specially designed levitation coil.

3.1. Measurement Coils

The magnetic field generated by a set of N concentric, thin current coils, located at distances r_n and angles θ_n (see Fig. 4) can be represented as an expansion in spherical harmonics. Only the zeroth-order term of this expansion describes the homogeneous part of the field. Thus, the requirement

that terms of order $k \geqslant 1$ have to disappear results in the following conditions on the coordinates (r_n, θ_n) of the coil windings

$$\sum_{n=1}^{N} \left(\frac{1}{r_n}\right)^k \sin\theta_n \, P_k^1(\cos\theta_n) = 0 \qquad \text{for all} \quad 2 \leqslant k \leqslant N+1 \tag{4}$$

the satisfaction of which yields a coil that generates a nearly homogeneous magnetic field. Here P_k^1 are the Legendre functions of first order and kth degree. Evidently, the N conditions of Eq. (4) result in a great amount of arbitrariness in the determination of the $2N$ coordinates (r_n, θ_n). We chose the N angular coordinates θ_n such that $\cos\theta_n$ corresponds to the N zeros of P_{N+1}^1. This satisfies Eq. (4) for $k = N+1$. The N radial coordinates are then (up to one) determined by the $N-1$ remaining equations of Eq. (4). With the help of the single undetermined radial coordinate, the extension of the coil can be arbitrarily fixed. For $N=2$ this procedure results in the well-known Helmholtz coil condition; see Fig. 4. But the more coil windings that are used, i.e., the higher N is, the more terms of the expansion can be set to zero and the better is the homogeneity of the resulting field. The measurement coil we use consists of eight windings with coordinates determined via the above mentioned procedure. Compared to a long, straight cylindrical coil, which also produces a homogeneous field, our coil provides a very compact arrangement around the sample, which gives, on the one hand, a better resolution of the signal from the sample and allows, on the other hand, the adjustment between the levitation coils shown in Fig. 5.

3.2. Levitation Coil

The essential function of the levitation field consists of the stable, contactless positioning and heating of the conducting sample. In addition, we require that the Lorentz force excerted on the sample shall simultaneously keep the liquid droplet as spherical as possible. For high-conducting samples and high field frequencies, where, due to the small skin depth δ [Eq. (2)], the field enters the sample only by a small amount, this condition is satisfied, if the magnetic field pressure on the sample surface just matches the hydrostatic pressure of a spherical droplet. This means

$$\frac{|\mathbf{B}(R_0, \theta)|^2}{2\mu_0} = \rho g R_0 (1 - \cos\theta) \tag{5}$$

where ρ denotes the liquid sample density, g is the gravitational constant, and θ is the polar angle on the sample surface. Here, again, the square of the total magnetic field $|\mathbf{B}(R_0, \theta)|^2$ is expanded in Legendre functions with

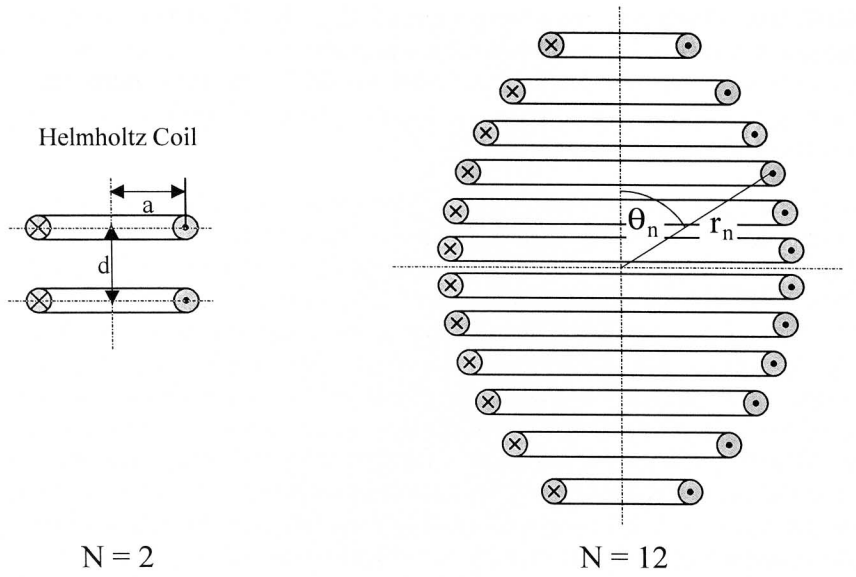

Fig. 4. Coils with 2 and 12 windings. The first coil, which satisfies the Helmholtz condition, $d = a$, produces a less homogeneous magnetic field near its center than the second coil.

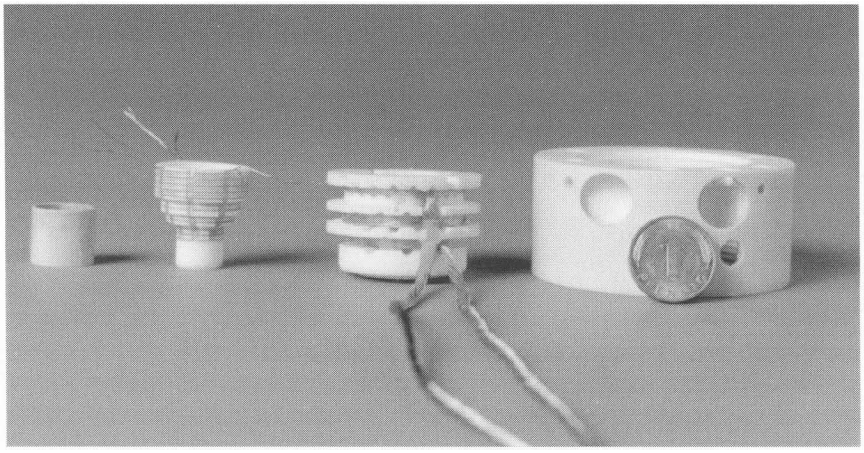

Fig. 5. Picture of (from left to right) the BN heat shield, the lower half of the measuring coil system, the lower half of the levitation coil (both fixed on a ceramic core), and the lower half of the outer ceramic housing. The parts are integrated within each other and cooled by circulating water.

coefficients fitting the right-hand side of Eq. (5). Since the coefficients depend on the location of the levitation coil windings, the fit gives conditions for their coordinates. However, the better the field expansion approximates Eq. (5), the worse its horizontal positioning stability becomes. So a good compromise has to be found (see Fig. 5).

4. MEASUREMENT FACILITY

4.1. Magnetic Field Control

As explained above there are two induction coil systems that mutually interact. Due to the very high levitation fields, high voltages are induced in the measurement coils. To prevent damage to the linked electronics, compensation transformers had to be added between the levitation and the measurement circuits. The voltages mutually transferred between the circuits via these transformers are just opposite to those induced by the coils, so that the levitation circuit and the measurement circuit are almost completely independent.

Nevertheless, there is still a residual voltage in the measurement circuit from the levitation field which could severely disturb the signals from the sample. This problem is circumvented by a periodic interruption of the levitation current for a few milliseconds. Within this time, which is short enough not to impact the positioning of the sample, the undisturbed electrical conductivity measurement is performed.

4.2. Arrangement of the Subsystems

Figure 6 shows a schematic diagram of the complete measurement facility. The main part consists of the levitation and measuring coil systems, and a third system for inductive detection of the vertical sample position, which is necessary because of the obstructed side view (see Fig. 5). For clarity the coils are drawn side by side. They are located in an ultrahigh vacuum chamber filled with inert gas. The gas is used to cool the levitated molten droplet to the measurement temperature. During the experiment the temperature is measured by a pyrometer looking from the top onto the sample. The data are continuously monitored by a computer. Integrated within this instrument is a videocamera which gives an optical view of the levitated droplet from above.

The levitation coil is powered by a levitation generator, which gives a trigger signal when the levitation power is interrupted. Then, via a sine wave function generator controlled by the computer, and a subsequent amplifier, the primary measurement coil, or alternatively the induction

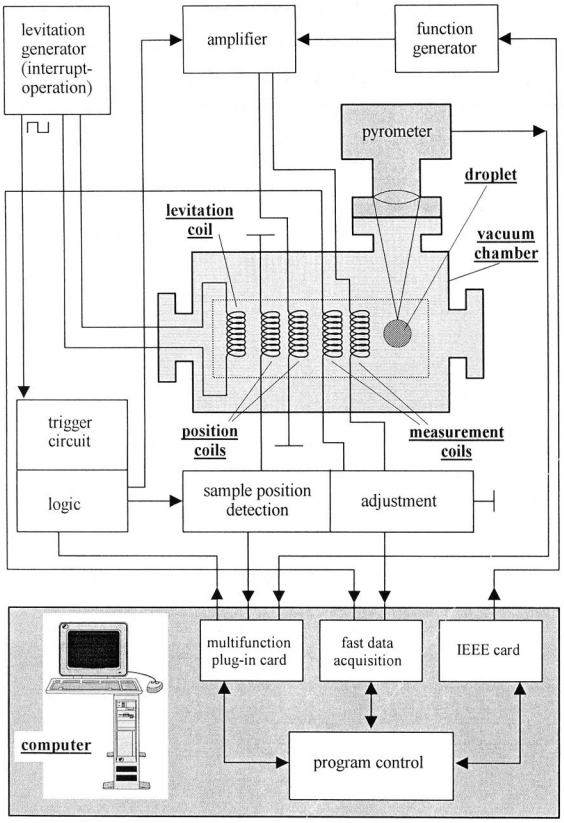

Fig. 6. Schematic arrangement of the facility subsystems.

coils of the sample position detection circuit, is powered. During this time the signals of either the secondary conductivity measurement coil or the position detection coil are monitored by the computer, after having passed adjusting electronics. The control of the whole experiment procedure is done by a computer, which also analyzes the data after the end of each experiment run.

5. SUMMARY

The major concern for electrical conductivity measurements of undercooled metallic melts is the avoidance of all mechanical contacts with the material under investigation. This makes a combination of a containerless positioning method, in our case electromagnetic levitation, with an inductive

conductivity measurement technique necessary. Up to now, this measurement technique has been applied only to low-melting metallic liquids contained in an ampoule that gives the material a well-defined cylindrical shape. We have extended this method to freely suspended liquid metals of nearly spherical shape. Meanwhile, we have essentially completed the construction of the above described facility, so that we are now ready to start the calibration measurements and the measurements of the electrical conductivity in the physically interesting undercooled regime of the metallic melts.

REFERENCES

1. T. Iida and R. I. L. Guthrie, *The Physical Properties of Liquid Metals* (Clarendon Press, Oxford, 1988).
2. W. Haller, H.-J. Güntherodt, and G. Busch, *Inst. Phys. Conf. Ser.* **30**:207 (1977).
3. I. Egry, G. Lohöfer, and S. Sauerland, *Int. J. Thermophys.* **14**:573 (1993).
4. E. C. Okress, D. M. Wroughton, G. Comenetz, P. H. Brace, and J. C. R. Kelly, *J. Appl. Phys.* **23**:545 (1952).
5. G. Lohöfer, *SIAM J. Appl. Math.* **49**:567 (1989).
6. B. Delley, H. U. Künzi, and H.-J. Güntherodt, *J. Phys. E Sci. Instrum.* **13**:661 (1980).
7. Ya. A. Kraftmakher, *Meas. Sci. Technol.* **2**:253 (1991).
8. J. E. Enderby, S. Ansell, S. Krishnan, D. L. Price, and M.-L. Saboungi, *Appl. Phys. Lett.* **71**:116 (1997).
9. G. Lohöfer, *Int. J. Eng. Sci.* **32**:107 (1994).